BROOKHAVEN
NATIONAL LABORATORY

BNL-77679-2007-CP

Effectiveness of electrostatic shielding and electronic subtraction to correct for the hole trapping in CdZnTe semiconductor detectors

A. E. Bolotnikov*, G. S. Camarda, A. Hossain, Y. Cui, and R. B. James

Brookhaven National Laboratory
Upton, NY 11793

SPIE – The International Society for Optical Engineering, 2007

Nonproliferation and National Security Department
Detector Development and Testing Division

Brookhaven National Laboratory
P.O. Box 5000
Upton, NY 11973-5000
www.bnl.gov

*bolotnik@bnl.gov; phone 631-344-8014; fax 631-344-3374

DISCLAIMER

Effectiveness of electrostatic shielding and electronic subtraction to correct for the hole trapping in CdZnTe semiconductor detectors

A. E. Bolotnikov*, G. S. Camarda, A. Hossain, Y. Cui, and R. B. James

Brookhaven National Laboratory
Upton, NY 11973

ABSTRACT

CdZnTe (CZT) is a very promising material for nuclear-radiation detectors. CZT detectors operate at ambient temperatures and offer high detection efficiency and excellent energy resolution, placing them ahead of high-purity Ge for those applications where cryogenic cooling is problematic. The progress achieved in CZT detectors over the past decade is founded on the developments of robust detector designs and readout electronics, both of which helped to overcome the effects of carrier trapping.

Because the holes have low mobility, only electrons can be used to generate signals in thick CZT detectors, so one must account for the variation of the output signal versus the locations of the interaction points. To obtain high spectral resolution, the detector's design should provide a means to eliminate this dependence throughout the entire volume of the device. In reality, the sensitive volume of any ionization detector invariably has two regions. In the first, adjacent to the collecting electrode, the amplitude of the output signal rapidly increases almost to its maximum as the interaction point is located farther from the anode; in the rest of the volume, the output signal remains nearly constant. Thus, the quality of CZT detector designs can be characterized based on the magnitude of the signals variations in the drift region and the ratio between the volumes of the drift and induction regions. The former determines the "geometrical" width of the photopeak, i.e., the line width that affects the total energy resolution and is attributed to the device's geometry when all other factors are neglected. The latter determines the photopeak efficiency and the area under the continuum in the pulse-height spectra.

In this work, we describe our findings from systematizing different designs of CZT detectors and evaluating their performance based on these two criteria.

Keywords: CdZnTe, gamma ray detectors, weighting potential

1. INTRODUCTION

CdZnTe (CZT) has great potential as a detection medium for nuclear-radiation detectors, because it operates at ambient temperatures, provides high detection efficiency and excellent energy resolution, and can be processed by using robust semiconductor technologies. In many practical applications, these advantages place CZT material ahead of high-purity Ge (HPGe) even though its intrinsic energy resolution is slightly worse. In contrast to HPGe which requires cryogenic cooling, CZT detectors are finding their niches in practically all areas where x-and gamma radiation must be detected, such as astronomy, medical- and industrial- imaging, national security, and personal dosimeters [1].

In the past decade, new detector designs and readout electronics developed for CZT detectors have afforded the means to overcome the effects of uncollected holes and electron trapping, and further improvements in CZT crystal growth have yielded high-homogeneity material with small concentrations of defects, and consequently, high mobility-lifetime products [2-5].

* bolotnik@bnl.gov; phone 631-344-8014; fax 631-344-3374

Because of the low mobility of the holes, only electrons can be used to generate signals in thick CZT detectors. For detectors that rely on collection of both electrons and holes, the amplitude of the output signal depends on the location of the interaction point, which adversely affects the energy resolution. This problem is common to most wide band-gap semiconductor detection materials and can be overcome by using special detector designs. However, the influence of the holes cannot be eliminated completely for the entire sensitive volume of the device. In practice, the device's sensitive volume invariably has two regions associated with fast and slow variations of the output signals. To characterize the quality of the electron-transport-only designs of CZT detectors, we used the terminology originally applied to classic gas-ionization chambers [6]. Accordingly, the region adjacent to the collecting electrode (anode) is called the induction region, in which the amplitude of the output signal rapidly increases from zero to near maximum as the location of the interaction point moves farther from the anode; and the rest of the volume is the so-called drift region, in which the output signal remains nearly constant. An imaginary surface dividing these two regions can be defined as the points at which the output signal decreases by a certain percentage of its maxima. Therefore, two criteria characterize the quality of the CZT detector's design: 1) The magnitude of the variations of the output signals in the drift region; and, 2) the ratio between the volumes of the drift and induction regions. The former determines the "geometrical" width of the photopeak, i.e., the line width that determines the total energy resolution and is attributed to the device's geometry after neglecting all other factors. The latter determines the photopeak efficiency and the area under the continuum in the pulse-height spectra.

Two more factors contribute to the energy resolution of the CZT detectors: electronic noise, and fluctuations of the collected charge resulting from non-uniform distribution of the electron traps. Two examples of the latter are the local variations of the mobility-lifetime products, and microscopic defects with a high concentration of traps, such as Te inclusions.

The goal of this work is to systematize the CZT designs and evaluate their performance based on these criteria.

2. TWO BASIC APPROACHES TO CZT DETECTOR DESIGNS

CZT detectors are typically single-carrier devices for which only fast-moving electrons can be collected to determine the total number of electron-hole pairs produced by incident gamma-rays or other ionizing particles. As discussed in the introduction, their main drawback is that the amplitude of the output signal is affected by the uncollected holes and, as a result, the signal depends on the locations of interaction points inside the detector. Such dependence is termed the induction effect and exists in many ionization detectors, e.g., gas-ionization chambers. This effect hinders the spectral resolution of single-carrier detectors unless special designs are employed to eliminate, or at least minimize, it.

Despite a large variety of designs for CZT detectors, they all rely only on two approaches to eliminating the effect of the holes. This follows from the general equation for the amplitude of the output signal A_{out} in the ionization detectors, which can be written as

$$A_{out}=Q_{col}+Q_{ind}, \tag{1}$$

where Q_{col} is the total collected charge, and Q_{ind} is the total charge induced on this electrode by the uncollected carriers. Here, we assume that the decay time of the readout preamplifier is much longer than the carriers' drift time. A_{out} is measured in units of collected charge. Eq. 1 is founded on very basic considerations; the term Q_{col} reflects the fact that for every charge actually reaching the electrode, an identical image charge appears on the electrode, while the term Q_{ind} represents the image charge induced by all the uncollected charges. Also, the equation can be accurately derived from the Shockley-Ramo theorem [7,8]. Let us assume that N_0 electron-hole pairs initially are generated at a point "O" for which the weighting potential is φ_0. By the time that the electrons reach the contacts or become trapped, the total induced signal on the collecting electrode will be given by

$$A_{out} = N_0 - N_e + \sum_{i=1}^{N_e}\varphi_i^e - N_0\varphi_0 - \left(\sum_{i=1}^{N_h}\varphi_i^h - N_0\varphi_0\right) = N_0 - N_e + \sum_{i=1}^{N_e}\varphi_i^e - \sum_{i=1}^{N_h}\varphi_i^h, \tag{2}$$

where φ_i^e and φ_i^h are the weighting potentials at the locations where the electrons and holes became trapped, and N_e and N_h are the total numbers of trapped holes and electrons. The difference $N_0 - N_e$ gives the total number of collected electrons for which the weighting potentials equal 1. Eq. 2 does not include the holes and electrons collected by

other electrodes since their weighting potentials are 0. The terms $N_0\varphi_0$ are cancelled, and the only terms left are the total collected charge Q_{col} and the total charge induced by the trapped holes and electrons Q_{ind} (holes have the opposite charge), i.e., Eq. 2 becomes Eq. 1.

Thus, the primary goal of any detector design is to eliminate (or minimize) the second term, Q_{ind}, in Eq. 1. (In some cases, Q_{col} can also depend (weakly) on the location of the interaction points due to electron trapping, and, as a result, both dependences can compensate each other.) There are two ways to do this: 1) Electrostatically shield a collecting electrode from the effect of the holes; and, 2) electronically subtract the charge signals induced by the hole. In practice, it is impossible to shield (or subtract) the effect of the uncollected holes completely throughout the entire active volume of the device. Again using the terminology applied to classic Frisch-grid gas-ionization chambers, the residual effect of the uncollected holes in CZT detectors can be described as the *inefficiency* of the design to shield from or subtract the effect of the holes.

This inefficiency in design to shield from or subtract Q_{ind} directly contributes to the geometrical width of the photopeak and can be measured as a percentage of the photopeak's width relative to its position. As discussed earlier, almost inevitably the active volume of a single-charge carrier ionization detector has two regions: the drift region, in which the device's response weakly depends on the location of the interaction points; and, the induction region, in which the amplitude of the output signal changes from maximum value to zero. In the special case of classic Frisch-grid ionization chambers [9], the amplitude of the output signals changes as a linear function of one of the coordinates (e.g., z-coordinate) in both regions. Then, the shielding inefficiency in the detector's design (Frisch-grid) is defined as a percentage of the total drop of the signal over the drift region. Assuming that the interaction points are uniformly distributed inside the detector's volume, the relative geometrical width of the photopeak will exactly equal shielding inefficiency.

In general, the dependence of the output signal in CZT detectors is more complex, but always can be approximated with two linear functions, while the division between the induction and drift regions can be defined as the point in the Z-direction at which the output signal decreases by a certain percentage of its maxima. Another important factor is the loss in collected charge due to continuous electron trapping by point defects. Electron trapping reduces the amplitude of the output signal proportionally to the drift distance, which compensates for the effect of the inefficiency of shielding/subtracting. Thus the actual variation in the output signals in the drift region results from the interplay between the inefficiency of shielding/subtraction and the electron trapping, both of which depend upon the device's geometry. In a good design, the variations of the output signals in the drift region are small, and the volume of this region is much greater than that of the induction region. We note that in several designs the variation of the output signals in the drift region can be corrected, while the events interacting in the induction region can be rejected by measuring the coordinates of the interaction points.

The shielding/subtraction inefficiency of a design imposes an intrinsic limit on the best-achievable energy resolution. The total energy resolution of the ionization detector is set by a combination of three factors: electronic noise, geometrical width, and fluctuations of the collected charge due to the non-uniform distribution of the electron traps. Two examples of such non-uniform distribution are the local variations in the electron mobility-lifetime product, and microscopic defects, such as Te inclusions, with a high concentration of localized traps. Again, the latter fluctuations can be corrected by using the coordinate information of the interaction points and by calibrating the device before its use. However, the fluctuations due to microscopic defects, like Te inclusions, cannot be corrected.

The side surfaces have an important role in CZT detectors. The drift line can be terminated on the side surfaces before reaching the collecting electrodes, resulting in the signal loss for the events interacting near the device edges. To avoid this effect the electrostatic potential on the surfaces should decrease slower than that inside the bulk. This will ensure that the field lines will be focused towards the collecting electrodes.

And finally, the efficiency of designs always depends on the boundary conditions (other conducting electrodes placed near the side surfaces and the collecting electrodes). The shielding/subtraction inefficiency of the detector can be improved by placing contacting or non-contacting shielding electrodes on the device side surfaces. It should be mentioned that the non-contacting electrode cannot change the electric field distribution inside the device but can modify the surface conductivity like that for a field-effect transistor.

3. ELECTRONIC SUBTRACTION OF THE INDUCED CHARGE (COPLANAR-GRID DEVICES)

Miroshnichenko *et al.* [10] proposed using electronic subtraction of the induced charge for multi-electrode detectors, wherein the induced charge Q_{ind} is determined by measuring the induced signals from one or several electrodes near the collected one. The electrodes can be composed of pixels or strips and, depending on the location of the interaction points, the same electrode can be used for measuring collected or induced-only charges. For example, for the pixel geometry, the signal from the collecting pixel can be corrected by subtracting the induced component interpolated using the induced signals measured from adjacent pixels. For strips, the induced charge Q_i^{ind} on a collecting strip "i" can be determined by reading signals Q_{i-1}, Q_{i+1}, Q_{i-2}, Q_{i+2}, and so on from two or more pairs of the adjacent ones. In the simplest case, a linear interpolation between two surrounding strips can be applied:

$$Q_i^{ind} = P\left(Q_{i-1} + Q_{i+1}\right), \tag{3}$$

where P is the weight depending on the device's geometry. Generally, subtracting the induced charge requires a rather complicated logic to identify the collecting electrode and evaluate the output signals. However, it can be simplified by using only two electrodes, and choosing their patterns in such way to ensure that the charges induced on both by the source-charge are equal. Moreover, collecting and non-collecting electrodes can be pre-defined by applying a negative bias on the latter electrode to generate an electric field that steers electrons toward the collecting one. Then, the contribution of the induced charge Q_{col}^{ind} to the total signal readout from the collecting electrode always equals to the induced signal Q_{non}^{ind} measured from the non-collecting grid. Thus, the device's output signal, defined as the difference between the signals' readout from the collecting and non-collecting grids A_{col}-A_{non}, equals the total collected charge Q_{col}^{col} that, in turn, is proportional to the energy deposited by the incident particle

$$A_{out}=A_{col}-A_{non}=\left(Q_{col}^{col}+Q_{col}^{ind}\right)-Q_{non}^{ind}=Q_{col}^{col}. \tag{3}$$

Luke [11] employed this approach in his so-called coplanar-grid (CPG) detector in which two coplanar grids consisting of interconnected strips subtracted the effect of the holes. Following his design, other geometries of coplanar electrodes were proposed [12]. Applying the CPG design to large-volume CZT crystals led to robust detectors with high detection efficiency and high energy resolution in a gamma-ray region. The magnitudes of energy resolution measured for different types of coplanar-grid detectors always were larger than the limits that could be explained from the Fano-factor and electronics noise; the best reported value was 1.2% at 662 keV [13]. Such discrepancies can be attributed to the inefficiency of electronic subtraction of the induced signal, and to the variations in the collected charge, both related to the grid designs. In other words, in real devices the grids are not exactly symmetrical and the difference $Q_{col}^{ind} - Q_{non}^{ind}$ is not negligible.

As an example, we consider the most popular design of CPG detectors, employing coplanar grids made of parallel strips, which several vendors offer. They generally incorporate the so-called third generation of the coplanar grids [14], and all exhibit the same intrinsic non-uniformities related using a one-dimensional grid pattern. Therefore, the amplitude of their output signal (difference A_{col}-A_{non}) slightly depends on the relative positions of the interaction points with respect to the nearest strip, and can be considered as local variations of the device's response. Although small, ~1% at 662 keV, such variations observed in the responses of CPG devices (Fig. 1) measured with collimated beams of X-rays and alpha particles [15], were attributed to different drift paths of the electron clouds and periodic lateral changes in the grid's weighting potentials [16-18]. These local variations of the output signal are superimposed on a slowly changing function caused by deviations in the grid's symmetry near the device's edges. Several generations of grid patterns were proposed to minimize the latter dependence [14], but less attention has been paid to the former.

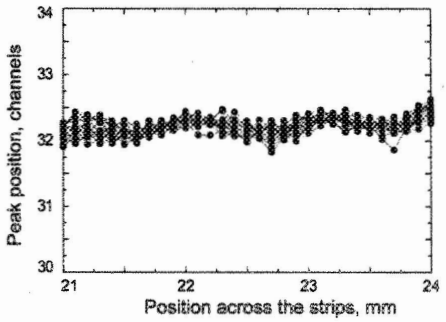

Fig. 1. Variations of the CPG device's response during the movement of a collimated X-ray beam across the strips [16].

The specific features of the CPG device's performance can be revealed by exploring the correlation between the amplitudes of the output signals from the collecting and non-collecting grids [18-19]. For example, Fig. 2 shows the correlation measured for a 15x15x7.5 mm^3 CPG device equipped with the "third-generation" [14] grid patterns comprised of 350-μm-wide strips pitched at 700 μm. The cathode and non-collecting grid were biased at -1000 and -60 V, correspondingly. The data measured with and without the differential bias applied between the grids is plotted in a two-coordinate system: A_{col} vs. A_{non} and A_{col}-A_{non} vs. A_{col}+A_{non} (a 45-degree rotation of a coordinate system). The detector was flood-illuminated with gamma rays from a ^{137}Cs source.

The correlation plots help to us to understand the details of the performance of CPG devices [18-19]. The distributions in Fig. 2 represent the superposition of several local correlation plots, each associated with two adjacent strips. As described before, global variations of grids' responses are important only for interaction events near the edges, while the local correlation plots should be nearly identical. Several important features emerge from the correlation plots. The narrow continuum of dots (track) corresponding to full-energy deposition events follows a straight line. The Compton edge is apparent in the distributions as an abrupt change in the density of the dots parallel to the distribution of total energy-deposition events.

Fig. 2 clearly indicates that the tracks of the total energy absorption events (the dots) are slightly off from a 45-degree (in the A_{col} vs. A_{non} coordinates) or 90-degree (in the A_{col}-A_{non} vs. A_{col}+A_{non} coordinates) angle with respect to the vertical axis, as would be expected for an ideal device. This deviation reflects charge loss due to electron trapping. In the first approximation, the positions of the actual tracks follow the lines $|A_{col}-\alpha A_{non}|=Q_0$ or $|(A_{col}-A_{non})+\alpha(A_{col}+A_{non})|=Q_0$, where α is a numerical coefficient related to the electron mobility-lifetime product, and Q_0 is the energy of the gamma rays. The first condition justifies Luke et al.'s proposed relative gain compensation techniques [20-21] to correct for the electron loss due to trapping. Using the charge conservation law $A_{col}+A_{non}-A_{cath}=0$, where A_{cath} is the amplitude of the cathode signal, the second condition can be re-written as $|(A_{col}-A_{non})+\alpha A_{actl}|=Q_0$, that justifies another correction technique proposed by He et al. [22-23].

Another notable feature in Fig. 2 is the broadening of the distributions of the total energy-deposition events (the dots) for interaction events taking place deep inside the detector. This is attributed to the asymmetrical grids' responses near the edges that shift energy deposition upward or downward, thereby symmetrically broadening its track. Such events contribute to the long tails present on both sides of the photopeaks in the pulse-height spectra measured from the CPG detectors. Moreover, the width of the energy deposition's distribution above the threshold where it starts to broaden cannot be entirely explained by electronic noise. Additional noise is generated by the local variations in the grids' signals caused by the local dependences of the collected charge and the grids weighting potentials as described above.

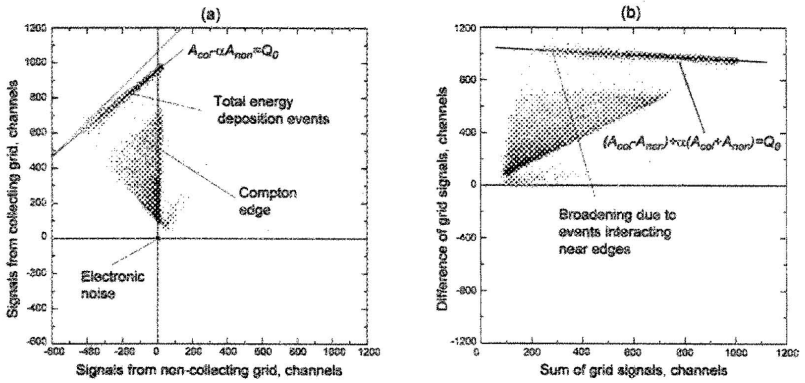

Fig. 2. Correlations between the grids signals plotted in two-coordinates systems: (a) A_{col} vs. A_{non}, and, (b) A_{col}-A_{non} vs. A_{col}+A_{non} (rotated 90 degrees).

To reduce the energy resolution in CPG detectors below 1%, the subtraction efficiency of the grids should be improved, while, at the same time, minimizing the variations of the collected charge caused by one-dimensional grids. For example, more symmetrical grids patterns with smaller features can be employed; however, the latter may raise the grids' capacitance too much and result in high electronic noise. The uniformity of the response of current generations of the coplanar-grids near their edges can be bettered by adding an extra non-collecting strip, so that every collecting strip will lie between two non-collecting strips. Further, two non-collecting grids might be placed in such a way that each collecting strip is enclosed between two non-collecting strips from different grids; then, the signal from the two non-colleting grids must be added together. In addition, these strips can be used to correct local- and global-variations in the device's response. We note that boundary conditions can significantly modify a device's response near its edges; any electrodes placed near or around the detector will help to reduce the device's shielding/subtracting inefficiency, and thus improve its performance. Another approach would be to use the pixel pattern wherein contacts are connected via their diagonal corners to form two coplanar grids, so that the alternating grid pattern spreads in two directions. We are currently investigating these approaches to improve the performance of a CPG detector.

4. ELECTROSTATIC SHIELDING OF THE EFFECT OF THE HOLES: PIXEL AND VIRTUAL FRISCH-GRID DETECTORS

Frisch [24] originally suggested electrostatically shielding the electron-collecting electrode from the effect of positive ions for gas-ionization chambers. In the classic version of the chamber a metal grid, called the Frisch-grid, lies inside the sensitive volume of the detector. However, if the conducting electrodes are placed outside the sensitive volume, they also have the same shielding effect as if a real Frisch-grid were installed inside the detector. Therefore, such devices are termed "virtual" Frisch-grid detectors. Previously, such designs were proposed for gas-ionization chambers and more recently for CZT and other compound semiconductor detectors, such as CAPture™ [25], hemispherical [26], Frisch-ring [27-28], and pixel [29] detectors.

4.1. Pixel detectors

Pixel detectors represent the most advantageous way to utilize all the benefits offered by CZT material: excellent energy resolution, sub-millimeter spatial resolution (the most desired attributes of CZT detectors), high stopping power, and the ability to correct material non-uniformities and electron trapping.

In pixel detectors, the charge induced on a particular pixel by the uncollected holes is shielded by other pixels. In the first approximation, the induced charge per pixel decreases proportionally to the total number of pixels so affording very effective electrostatic shielding of every pixel; this is called the small pixel effect [29]. Because of the two-dimensional

periodic pattern and small sizes of the pixels, the induction region in pixel detectors can be very narrow, allowing the entire volume of the crystal to be utilized.

Let us consider the commercial 10x10x10 mm^3 4x4 pixel detector with a pixel size of 2.5x2.5 mm^2 available from eV Products, Inc. The detector has relatively large pixels, which make it easer to see the shielding inefficiency associated with pixel designs. Fig. 3 illustrates this device's performance, showing the distribution of the signal amplitudes' readout from a particular pixel versus drift time. The drift time provides information on the interaction depth for single interaction point events that constitute the majority of events measured by a small-area pixel. As seen, the dots representing the total energy deposition events are concentrated along the curve that bends toward low amplitudes in the induction region corresponding to events interacting close to the anode side. The curve is almost flat in the drift region indicating a nearly perfect compensation for the inefficiency of shielding that this particular pixel pattern provides by trapping electrons. In contrast, the distribution of the negative amplitudes induced by the holes when the electrons are collected by other pixels has a positive slope, which illustrates the effects of shielding inefficiency.

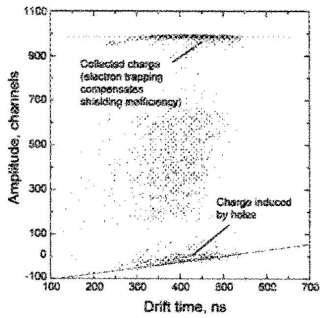

Fig. 3. Distribution of the amplitudes of the signals read out from a representative pixel versus the drift times measured for a 10x10x10 mm^3 4x4 pixel detector.

For the detector used in this example, the interacting events in the induction region (close to the anode) cause asymmetrical widening and low-energy tailing of the peaks in the pulse-height spectra. Nevertheless, the pixel's geometry offers several ways to correct this. The simplest is to use smaller pixels, which will improve the shielding efficiency and reduce the induction region. Another way is to subtract the unwanted extra charge induced on the pixel, due to inefficient shielding, by the amplitudes of readout from the signals from adjacent pixels. But perhaps the most effective approach is to apply an interaction-depth-sensing technique to measure the z-coordinates of the interaction points. This method enables the pixel detectors to operate in a time projection chamber (TPC) mode, which is the most effective way to simultaneously correct all three effects: the inefficiency of shielding, electron trapping, and the variations of the collected charge due to some material non-uniformities [30]. Employing this approach, Zhang et al [31] achieved an energy resolution of <1% at 662 keV in large, 15x15x10 mm^3, CZT pixel detectors.

4.2. Virtual Frisch-grid detectors based on bar-shaped crystals

Recently, the virtual Frisch-grid devices that utilize bar-shaped crystals have was proposed by McGregor and Rojeski [27] and Montemont et al. [28] and named, respectively, Frisch-ring and Capacitive Frisch-grid detectors. The rectangular (or bar-shape) geometry of these devices, typically 5x5 mm^2 with thickness up to 20 mm, offer several benefits, viz. low cost, easy to produce, and high stopping power, which makes them very attractive for position-sensitive CZT arrays.

In contrast to CAPture™ or hemispherical detectors in which the cathode electrode extends up the sides of the detector body, the Frisch-ring devices use a shielding electrode that is physically separated from the semiconductor's surfaces by a thin layer of insulating material. This electrode, the main feature of the devices that McGregor and Rojeski [27] termed non-contacting Frisch-ring, distinguishes them from CAPture™ and hemispherical-type devices. In the simplest practical realization of this device [32], the non-contacted electrode also was an extension of the cathode.

The shapes of the signals generated on the anode of the Frisch-ring device are similar to those produced in pixel detectors. Accordingly, the Frisch-ring device can be considered as a single segment of the pixel detector. Kargar et al. [33] and Bolotnikov et al. [34] investigated the optimal geometry and performance limits of the Frisch-ring design. They found theoretically, and confirmed experimentally, that such devices with geometrical aspect ratios (the width-to-thickness ratio) of <0.5 potentially can attain an energy resolution of <1% FWHM at 662 keV and the peak-to-Compton ratio of ~5. Furthermore, surface preparation and shielding were very critical for assuring the best performance. Provided that they are properly dealt with, the device's performance is limited only by electron trapping. Fig. 4 depicts the simulated lateral variations of the responses of a 5x5x14 mm^3 Frisch-ring device for events interacting at three distances, 2-, 4-, and 7-mm above the anode. We show only one quarter of the device: the beginning of the coordinate system is located at the device's center. In our calculations, we took into account an exact weighing potential and the electron loss due to trapping ($\mu\tau$=10^{-2} cm^2/V).

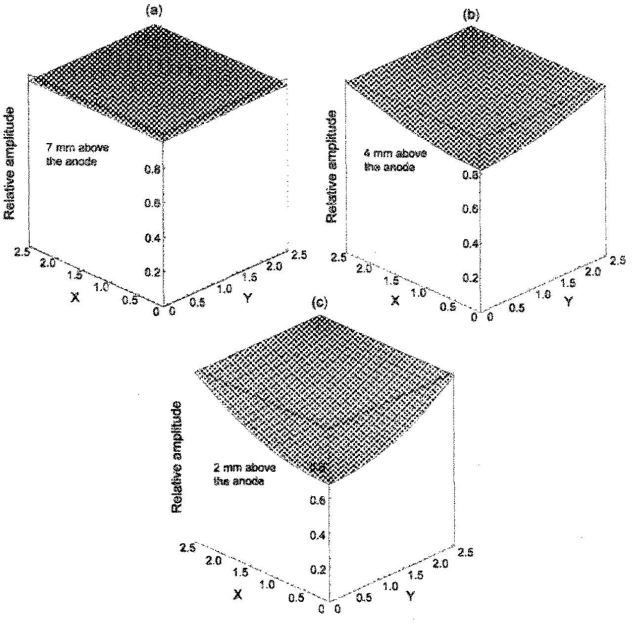

Fig. 4. Lateral variations of the 5x5x14 mm^3 Frisch-ring detector's response calculated for events interacting at (a) 7 mm, (b) 4 mm, and, (c) 2 mm above the anode. The coordinate system is located in the center of the detector. Only a quarter of the device is shown, and the x- and y-axis represent distances, in mm, from the device's center.

As seen, the device's response at ~5 mm above the anode varies slightly due to electron trapping. Below this level, both the lateral- and depth-variations of the weighing potential are significant, meaning that a substantial part of the device's volume is wasted. This fact also is reflected in the amplitude versus drift-time distributions measured and simulated for the device with the same geometry (Fig. 5). The cathode bias was 1800 V. To make the simulated distribution and the measured one comparable, we adjusted the μτ-product ($2.5x10^{-2}$ cm^2/V) and assumed a linearly decaying electric field inside the detector (a reduction in field-field strength of ~25%).

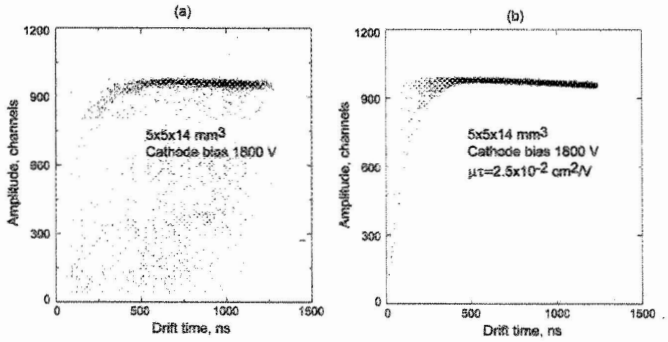

Fig. 5. Amplitude versus drift-time distribution measured (a) and simulated (b) for the 5x5x14 mm3 Frisch-ring detector. The cathode bias is 1800 V. To make the simulated distribution and the measured one comparable, we adjusted the μτ-product ($2.5x10^{-2}$ cm^2/V) and assumed a linearly decaying electric field inside the detector (a reduction in electric field strength of ~25%).

In general, the theoretical curve reproduces the shape of the measured distribution. However, there are some discrepancies. First, the actual drift time is ~30% longer than the calculated value based on our assumption of a uniform electric field inside the crystal slab. Only by integrating the linear decrease in field strength from the cathode toward the anode were we able to accurately reproduce the measured curve. Second, the experimental distribution shows no events interacting in the induction region close to device's surfaces, suggesting that for such events electron trapping near the surface results in a complete loss of charge. The induction region in Frisch-ring detectors extends up to ~5 mm above the anode, and its fraction of the total device's volume is substantially greater than those in CPG and pixel detectors. This is a major drawback of current designs of the Frisch-ring detectors that needs further improvement.

5. CONCLUSIONS

We evaluated the performance of the basic designs of CZT detectors from the viewpoint of the residual effect of the uncollected holes in CZT detectors.

Although a great variety of the designs have been proposed for CZT and other semiconductor detectors operating in an electron-collection mode, they utilize only two ways for minimizing the effect of the uncollected holes; namely electrostatically shielding the collecting electrodes from the effect of the holes, or electronically subtracting the charge signals induced by the holes. In practice, it is impossible to completely shield (or subtract) the charge induced by the uncollected holes over the device's entire active volume.

In some designs for CZT detectors, the variation of the output signals in the drift region can be corrected, while rejecting the interaction events from the induction region, thus improving the device's performance. Furthermore, fluctuations of the output signals caused by smooth variations of the electron mobility-lifetime product can be corrected in designs that provide coordinate information on the interaction points.

The device's side surfaces play an important role in CZT detectors. The drift-lines can be terminated by the side surfaces before reaching the collecting electrodes resulting in a loss of signal for interacting events near the edges. To avoid this effect the electrostatic potential on the surfaces should decrease more slowly than that in the bulk; this will ensure that the field lines are focused towards the collecting electrodes.

Finally, the efficiency of designs always depends on the boundary conditions. While other conducting electrodes can be placed near the side surfaces and the collecting electrodes, the contacting or non-contacting shielding electrodes must always be sited on the device's side surfaces to improve the efficiency of shielding/subtraction.

ACKNOWLEDGEMENTS

This work was supported by U.S. Department of Energy, Office of Nonproliferation Research and Engineering, NA-22. The manuscript has been authored by Brookhaven Science Associates, LLC under Contract No. DE-AC02-98CH1-

886 with the U.S. Department of Energy. The United States Government retains, and the publisher, by accepting the article for publication, acknowledges, a world-wide license to publish or reproduce the published form of this manuscript, or allow others to do so, for the United States Government purposes.

REFERENCES

[1] R. B. James, T. E. Schlesinger, J. C. Lund and M. Schieber, "Cadmium Zinc Telluride Spectrometers for Gamma and X-Ray Applications", in Semiconductors for Room Temperature Nuclear Detector Applications, Vol. 43, edited by R. B. James and T. E. Schlesinger (Academic Press, New York, 1995), p. 334.

[2] A. Owens and A. G. Kozorezov, "Single carrier sensing techniques in the compound semiconductor detectors," *Nucl. Instr. Meth.* A 563, pp. 31-36, 2006.

[3] P. J. Sellin and J. Vaitkus, "New materials for radiation hard semiconductor detectors," *Nucl. Instr. Meth.* A 557, pp. 479-489, 2006.

[4] C. Szeles, S. E. Cameron, J.-O. Ndap, and W. C. Chalmers, "Advances in the crystal growth of semi-insulating CdZnTe for radiation detector applications", *IEEE Trans. Nucl. Sci.*, NS 49, n.5, pp. 2535-2540, 2002.

[5] H. Chen, S. Awadalla, R. Redden, G. Bindley, A. Bolotnikov, G. Camarda, G. Carini and R. B. James "High-performance, large-volume THM CdZnTe detectors for medical imaging and homeland security applications," submitted to *IEEE Trans. Nucl. Sci.*,2007.

[6] G. F. Knoll, *Radiation Detection and Measurement*, 3rd ed. 2000, New York: John Wiley & Sons, Inc.

[7] S. Ramo, *Proc. IRE* 27, p.584, 1939.

[8] W. Shockley, *J. Appl. Phys.* 9, p.635, 1938.

[9] O. Buneman, T. E. Cranshaw, and J. A. Harvey, "Design of Grid Ionization Chambers," *Can. J. Res.*, A27 (1949) pp. 191-206.

[10] V. P. Miroshnichenko, B. U. Rodionov, and E. Shuvalova, "The method of detection of gamma radiation", USSR Patent SU-1264723A, issued June 15, 1986.

[11] P. N. Luke, "Single-polarity charge sensing in ionization detectors using coplanar electrodes", *Appl. Phys. Lett.* 65 (22), pp. 2884-2886, 1995. Also see US Patent 5,530,249 by P. N. Luke (1996).

[12] T. Prettyman, M.K. Smith, S.E. Soldner, "Design and Characterization of Cylindrical CdZnTe Detectors with Coplanar Grids", *Proc. SPIE* Vol. 3768, p. 339-347, Hard X-Ray, Gamma-Ray, and Neutron Detector Physics, Ralph B. James; Richard C. Schirato; Eds., 1999.

[13] eV Products, Inc. website: http://www.evproducts.com.

[14] Z. He, G. F. Knoll, D. K. Wehe, and Y. F. Du, "Coplanar grid patterns and their effects on energy resolution of CdZnTe detectors," *Nucl. Instr. Meth.* A 411, pp. 107-113, 1989.

[15] P. N. Luke, M. Amman, and J. S. Lee, "Factors affecting energy resolution of coplanar-grid CdZnTe detectors," *IEEE Trans. Nucl. Sci.* Vol. 51, pp. 1199-1203, 2004.

[16] G. A. Carini, A. E. Bolotnikov, G. S. Camarda, G. W. Wright, G. De Geronimo, D. P. Siddons, and R. B. James, "Synchrotron radiation response characterization of coplanar-grid CZT detectors," *IEEE Trans. on Nucl. Sci.* Vol. 52, pp. 1941-1945, 2005.

[17] A.G. Kozorezov, A. Owens, A. Peacock, and J.K. Wigmore, Carrier dynamics and resolution of co-planar grid radiation detectors," *Nucl. Instr. Meth. Phys. Res.* A 563, pp. 37-40, 2006.

[18] G. A. Carini, A. E. Bolotnikov, G. C. Camarda, G. W. Wright, and R. B. James "Non-uniformity effects in CdZnTe coplanar-grid detectors," accepted by Physica Status Solidi, 2007.

[19] A. E. Bolotnikov, G. S. Camarda, G. A. Carini, M. Fiederle, L. Li, G. W. Wright, and R. B. James, "Performance Studies of CdZnTe Detector by Using a Pulse-Shape Analysis", Invited Paper, in Proceedings of SPIE Hard X-Ray and Gamma-Ray Detector Physics VII, edited by R. B. James, L. A. Franks, and A. Burger (SPIE, Bellingham, WA, 2005), 59200K-1 – 59200K-12.

[20] P. N. Luke, "Electrode configuration and energy resolution in gamma-ray detectors", *Nuclear Instruments and Methods in Physics Research A* 380 (1996) 232-237.

[21] M. Amman and P. Luke, "Optimization criteria for coplanar-grid detectors", IEEE Trans. Nucl. Sci., vol. 46, pp. 205-212, 1999.

[22] Z. He, G. F. Knoll, D. K. Wehe, R. Rojeski, C. H. Mastrangelo, M. Hamming, C. Berret, and A. Uritani, "1-d position-sensitive single carrier semiconductor detectors", *Nucl. Instr. Meth. Phys. Res.* A 380 (1996), 228-231.

Formatted: English (U.S.)

[23] Z. He and B. W. Sturm, "Characteristics of depth-sensing coplanar grid CdZnTe detectors," Nuclear Science Symposium Conference Record, 2003 IEEE, Vol. 5, pp. 3601-3605, 2003.
[24] O. R. Frisch, Unpublished report, BR-49, "isotope analysis of uranium samples by means of their alpha-ray groups. British Atomic Energy Project, 1944.
[25] K. Parnham, C. Szeles, K. G. Lynn, and R. Tjossem, "Performance Improvement of CdZnTe Detectors Using Modified Two-Terminal Electrode Geometry," Hard x-ray, Gamma-Ray and Neutron Detector Physics, Proceedings of SPIE, Vol. 3786, pp. 49-54, 1999.
[26] V. Ivanov, P. Dorogov, R. Arlt, "Development of Large Volume Hemispheric CdZnTe Detectors for Use in Safeguards Applications", ESARDA Symposium on Safeguards and Nuclear Material Management, Proceedings, p. 447, Montpellier, France,13-15 May 1997.
[27] D. S. McGregor and R. A. Rojeski, U.S. Patent 6,175,120.
[28] G. Montemont, M. Arques, L. Verger, and J. Rustique, "A Capacitive Frisch Grid Structure for CdZnTe Detectors", *IEEE Trans. Nucl. Sci.*, vol. 48, pp. 278-281, 2001.
[29] H. H. Barrett, J. D. Eskin, and H. B. Barber, "Charge Transport in Arrays of Semiconductor Gamma-Ray Detectors", *Phys. Rev. Lett.* 75 (1), pp. 156-159, 1995.
[30] Z. He, W. Li, G. F. Knoll, D. K. Wehe, J. Berry, and C. M. Stahle, "3-D position sensitive CdZnTe gamma-ray spectrometers," *Nucl. Instr. and Meth. A* 422, pp. 173-178, 1999.
[31] F. Zhang, Z. He, D. Xu, G. F. Knoll, D. K. Wehe, and J. E. Berry, "Improved resolution for 3D position sensitive CdZnTe spectrometers," *IEEE Trans. Nucl. Sci.*, Vol. 51, pp. 2427-2431, 2004.
[32] W. J. McNeil, A.E. Bolotnikov, G. W. Wright, R. B. James, and D. S. McGregor, "Single Charge Carrier Type Sensing with a Frisch Ring CdZnTe Semiconductor Radiation Detector," *Applied Physics Letters*, 84, pp. 1988-1990, 2004.
[33] A. Kargar, A. M. Jones, W. J. McNeil, and D. S. McGregor, "CdZnTe Frisch Ring Detectors for Low-Energy Gamma Ray Spectroscopy," Nuclear Instruments and Methods, A558 (2006) pp. 487-503.
[34] A. E. Bolotnikov, G. S. Camarda, G. A. Carini, M. Fiederle, L. Li, D. S. McGregor, W. McNeil, G. W. Wright, and R. B. James, "Performance Characteristics of Frisch-Ring CdZnTe Detectors", *IEEE Trans. Nucl. Sci.*, vol. 53 (2), pp. 607-614, 2006.